RSC Advances

This is an *Accepted Manuscript*, which has been through the Royal Society of Chemistry peer review process and has been accepted for publication.

Accepted Manuscripts are published online shortly after acceptance, before technical editing, formatting and proof reading. Using this free service, authors can make their results available to the community, in citable form, before we publish the edited article. This *Accepted Manuscript* will be replaced by the edited, formatted and paginated article as soon as this is available.

You can find more information about *Accepted Manuscripts* in the Information for Authors.

Please note that technical editing may introduce minor changes to the text and/or graphics, which may alter content. The journal's standard Terms & Conditions and the Ethical guidelines still apply. In no event shall the Royal Society of Chemistry be held responsible for any errors or omissions in this *Accepted Manuscript* or any consequences arising from the use of any information it contains.

ROYAL SOCIETY OF CHEMISTRY

www.rsc.org/advances

Amorphous carbon modified nano-sized tungsten carbide as gas diffusion electrode catalyst for oxygen reduction reaction

Zhiwei Liu [a], Ping Li [a]*, Fuqiang Zhai [b], Qi Wan [c],

Alex A.Volinsky [d], Xuanhui Qu [a]

[a] Institute for Advanced Materials and Technology, University of Science and Technology Beijing, Beijing 100083, China.

[b] Departament Física Aplicada, EETAC, Universitat Politècnica de Catalunya - BarcelonaTech, 08860 Castelldefels, Spain.

[c] Energy Material & Technology Research Institute, General Research Institute for Nonferrous Metal, Beijing 100088, China.

[d] Department of Mechanical Engineering, University of South Florida, Tampa, FL 33620, USA.

Abstract

Nanostructured tungsten carbide with the high surface area, and containing amorphous carbon, is prepared by a low temperature combustion synthesis method. Nanostructured tungsten carbide is used as the catalyst for the gas diffusion electrode. The obtained WC with different carbon contents was investigated by XRD, FESEM, TG-DTA, BET and XPS. When the molar ratio of C/W is 19/3, the WC particles with different carbon contents are obtained after the carbonizing process between 900-1400 °C, and the content of free carbon in WC also increases gradually with temperature. Carbon content is tested by high frequency combustion-infrared absorption method in the carbon sulfur analyzer. The electrochemical properties of

Corresponding author: ustbliping@126.com (P. Li)
Tel: +86-10-82377286; Fax: +86-10-62334311.

RSC Advances Accepted Manuscript

tungsten carbide for the oxygen reduction reaction are characterized by polarization curves and electrochemical impedance. The results show that the presence of the appropriate amorphous carbon is beneficial for improving the conductivity and dispersibility of tungsten carbide catalyst, and more active centers can be provided by the catalyst.

Keywords: Low temperature combustion synthesis; Amorphous carbon; Electro-catalyst; Gas diffusion electrode.

1. Introduction

Metal-air batteries have aroused great interest due to the simple structure, non-polluting, high power and energy density. The cathodic oxygen reduction reaction (ORR) is one of the most important factors affecting the performance of a metal-air battery system. Among cathode catalysts for the metal-air battery, platinum is currently the most used electro-catalyst for the ORR [1-3], owing to its high chemical stability and electro-catalytic activity. Meanwhile, the disadvantages of high cost and easily poisoning by carbon monoxide [4] or methanol have greatly hindered the practical applications of metal-air battery. At present, searching for other novel substitutes, which could further improve the catalytic properties of oxygen electrodes has become a focal point of study in metal-air cells and fuel cells.

Nano-sized tungsten carbide (WC) is a new promising platinum-like catalyst for the gas diffusion electrode, not only due to its catalytic behavior close to platinum, but also its electrochemical stability, oxidation resistance and anti-poisoning are much higher than platinum catalysts [5-8]. Chen et al. [9] reported that WC is active to

RSC Advances Accepted Manuscript

methanol oxidation and is a promising alternative electrocatalyst at voltages up to ~0.8 V, WC also shows high potential for ORR due to its unique electron structure. Due to a good electronic conductivity, WC will become an excellent material for diffusion barrier layers in the field of semiconductors. Besides, WC can be used as a support material for the platinum catalyst [10], and the catalytic activity is also increased.

The presence of carbon on the WC surface has become a critical issue of using WC catalyst in electrochemical applications. The surface carbon will be present, unless it is properly controlled during the WC synthesis process, since the carbon source is derived from the decomposition of hydrocarbons [11, 12]. The influence of gas phase composition and synthesis temperature on the phases of W, W carbides and W oxides with and without surface carbon have been reported [13, 14]. Hara et al. [15] reported that the catalyst showed poor catalytic activity for hydrogen oxidation reaction (HOR) due to the surface carbon. In the study of ordered macroporous tungsten carbide, Bosco et al. [16] showed that surface carbon can stabilize the surface structure of WC, so the activity of methanol oxidation will be improved. In addition, Pt supported on mesoporous WC showed better catalytic performance for the hydrogen evolution reaction (HER) [17] and methanol electro-oxidation [18] than Pt supported on carbon, which is due to the free carbon present on the surface of WC.

In this work, WC precursor with the C/W molar ratio of 19/3 possessing higher catalytic properties was prepared by the low temperature combustion synthesis (LCS) method. The WC nanoparticles are obtained by the precursor after carbonization. The influence of different carbonization temperatures on the carbon content of WC was

RSC Advances Accepted Manuscript

studied. The electrochemical properties of nano-sized WC with different surface amorphous carbon content were characterized by polarization curves and electrochemical impedance measurements.

2. Experimental details

2.1 Preparation of WC catalyst

Mesoporous WC was synthesized by the LCS method, which is reported in the previous work [19]. Ammonium tungstate ($(NH_4)_{10}W_{12}O_{41}$), nitric acid (HNO_3, 65 wt.%), urea ($CO(NH_2)_2$) and glucose ($C_6H_{12}O_6 \cdot H_2O$) were used as raw materials in the synthesis of WC particles. First, 22.82 g of $(NH_4)_{10}W_{12}O_{41}$, 3 g of $CO(NH_2)_2$ and 18.81 g of $C_6H_{12}O_6 \cdot H_2O$ were dissolved together in 50 ml deionized water under stirring to obtain a redox mixture. Then, 9.69 g of HNO_3 were added to the solution and concentrated in a 500 ml beaker. The mixed solution was placed into a closed electric furnace in order to initiate a highly exothermic self-contained combustion process, resulting in production of a loose black WC precursor. Finally, the precursor was transferred into a tube furnace after grinding, where it was further carburized under argon flow at the 800 ℃ to 1400 ℃ temperature range for 6 h to obtain the samples. In order to conveniently describe the products of pure WC reduced and carburized at different temperatures, hereafter, these products are named as the catalyst A, B, C, D and E, corresponding to the reduction and carburization at 900 ℃, 1000 ℃, 1100 ℃, 1200 ℃ and 1400 ℃, respectively.

2.2 Samples characterization

The X-ray diffraction (XRD) measurements were carried out with a Rigaku

RSC Advances Accepted Manuscript

(D/MAX-RB) diffractometer using Cu Kα radiation (λ=1.5406 Å) at a scanning rate of 10º min^{-1}. The morphology and nanostructure of the samples were observed by using a field-emission scanning electron microscope (FESEM, Zeiss Ultra 55). Thermal stability of the sample was studied by TG-DTA (Seiko 6300) and the data were from room temperature to 1000 °C at a heating rate of 10 °C min^{-1} under air atmosphere. The BET (QuadraSorb SI) surface area measurement was calculated from nitrogen adsorption isotherms at -196 °C. The content of carbon element was measured by infrared absorption carbon-sulfur analyzer (CS-2008). Energy dispersive X-ray spectra (EDS) attached to the FESEM and X-ray photoelectron spectroscopy (XPS, ESCALAB 250 Xi) were also used to investigate the near surface chemical composition of the samples.

2.3 Gas diffusion electrodes preparation

Gas diffusion electrodes were prepared according to the earlier reports [20, 21], which consist of three layers: a catalyst layer, a gas diffusion layer and a current collecting layer. The preparation process of the catalyst layer can be described as follows: tungsten carbide, acetylene black and polytetrafluoroethylene (PTFE, 60 wt % suspension), according to the weight ratio of 3:5:2, were mixed in 20 ml of deionized water, and appropriate amount of anhydrous ethanol was added. The mixture would become a tough and sticky paste under magnetic stirring at 80 °C for 2 h. Under the pressure of 16 MPa, the paste was pressed into a size-specific catalyst layer by using a pellet press. The similar method was used to prepare the gas diffusion layer. The weight ratio of polytetrafluoroethylene to anhydrous sodium sulfate to acetylene black was

RSC Advances Accepted Manuscript

1:1:1. In the process, PTFE, anhydrous sodium sulfate and acetylene black were used as the binder, the pore former and the support material, respectively. Nickel foam was chosen as a current collector in the moisture barrier. The gas diffusion electrodes were obtained through pressing the three layers. At last, the electrodes were finished by sintering at 200 °C in nitrogen flow for 30 min. The loading amount of the active materials was 5 $mg \cdot cm^{-2}$. Pt (10 wt % Pt, Aladdin) gas diffusion electrode and activated carbon (AC) gas diffusion electrode were also prepared by following the same procedure as above.

2.4 Electrochemical characterization

Electrochemical measurements were carried out in a conventional three-electrode system using a Parstat 2273 electrochemical workstation at 30 °C. The nickel foil was used as the counter electrode and the prepared gas diffusion electrode was used as a working electrode. The area of the working electrode is 0.785 cm^2. Under alkaline conditions, Hg/HgO electrode was used as the reference electrode and the electrolyte was a 6 M KOH solution. Under neutral pH conditions, a saturated calomel electrode (SCE) was used as the reference electrode and the electrolyte was a 1 M NaCl solution. The steady state polarization curve measurements were conducted with a scan rate of 0.5 $mV \cdot s^{-1}$. The electrochemical impedance spectra (EIS) were recorded in the 0.01 Hz to 10 kHz ac signal range with 5 mV amplitude.

3. Results and discussion

3.1 Characterization of as-synthesized WC catalyst

The precursor of 19/3 C/W molar ratio was reduced and carburized at the different

RSC Advances Accepted Manuscript

temperature in argon atmosphere for 6 h, respectively. X-ray diffraction patterns of different samples are shown in Fig. 1. Obvious WC peaks and W_2C peaks appear when the temperature increases to 800 °C, suggesting that the carbonization reaction of the precursors had occurred. When the reduction carbonization temperatures is higher than 900 °C, strong WC peaks can be observed in Fig. 1, indicating that WO_3 completely transformed into pure WC through the carbonization process. According to the results calculated by the Scherrer formula, the average particle sizes of catalysts are 50.0 nm, 46.8 nm, 39.1 nm, 57.3 nm and 59.0 nm, which correspond to the catalyst A, B, C, D and E, respectively. Therefore, the carburization temperature affects the final WC phase generation.

Fig. 2 displays FESEM micrographs of the products prepared at different carbonization temperatures. A small amount of porosity appearing in the tungsten carbide samples results from a large amount of released heat during the low temperature combustion process. As shown in Fig. 2a-c, the particle sizes of the samples decrease with the rising of temperature. The particle size of catalyst lies in a wide range, and the agglomeration will happen during carbonization. When the carbonization temperature reaches 1100 °C, small size of the catalyst C can be obtained with homogeneous nano-sized particles with 40-50 nm. At the moment, the morphology of the WC particles has been transformed from the irregular to sphere, and the catalyst C has higher specific surface area. For further increasing the carbonization temperature, the tendency of powder agglomeration becomes more obvious and the particle size also tends to increase. The particle sizes of the catalyst D and the catalyst E

RSC Advances Accepted Manuscript

are both larger than the catalyst C, which is consistent with the XRD results.

The N_2 adsorption/desorption isothermal curves of the catalyst C are shown in Fig. 3. The sample exhibited the representative type IV isotherms with a distinct hysteresis loop over the P/P_0 ranging from 0.42 to 0.98, clearly showing the mesoporous properties of the prepared WC. In addition, the pore size distribution is shown in the inset of Fig. 3, demonstrating that the catalyst C is mesoporous with the maximum diameter of 3.84 nm. Based on the above analysis, it is reasonable to believe that the mesoporous structure of WC is suitable to use as a electrochemical catalyst material.

The specific surface area and the carbon content of the tested samples have been obtained, as shown in Table 1. The carbon content of all the samples is higher than the theoretical carbon content ($C/WC = 6.12$ wt %), suggesting the inevitable existence of free carbon in the final product, the free carbon content increases with the increase of carbonization temperature. The specific surface area of the catalyst B is slightly higher than the catalyst A due to the smaller particle size of the catalyst B. The surface profile will change when the carbonization temperature is higher than 1000 °C. The specific surface area of WC shows an increasing tendency with the rise of carbonization temperature. When the carbonization temperature increases to 1100 °C, the specific surface area of WC reaches 41.297 $m^2 \cdot g^{-1}$. However, with further temperature increasing, the specific surface area of WC will decrease due to the particles agglomeration.

Fig. 4 shows the thermogravimetry-differential thermal analysis (TG-DTA) of the catalyst C measured in an air atmosphere. The TG curve of the catalyst C has a

RSC Advances Accepted Manuscript

significant increase at 425 °C, which indicates that the weight of the sample has increased. The weight of the catalys C remains stable above 670 °C. The DTA curve shows that the exothermic reaction will occur between 425 °C and 670 °C for the catalyst C. The results show that the WC sample prepared by the low-temperature combustion synthesis method is stable under the temperature below 425 °C. When the temperature is higher than 425 °C, the WC sample will react with oxygen to produce tungsten oxide, meanwhile apparent heat is given off. It is consistent with the results of the literature [22].

Fig. 5 shows the XPS spectra for the surface composition of the catalyst A. As shown in Fig. 5a, the spectra of C1s in the catalyst A consists of a doublet with 284.68 eV and 282.7 eV binding energies, corresponding to amorphous carbon and WC. Fig. 5b shows the XPS spectra of W4f at 32.1 eV, 34.2 eV, and 38.1 eV, which are ascribed to WC, W_2C, and W_xO_y, respectively. The existence of W_xO_y explains that the exposed sample was oxidized in air. The elemental content of different surface products was characterized by XPS, as shown in Table 2. All tungsten carbide surfaces prepared at different carbonization temperatures have high oxygen content. The surface elemental content obviously changes with the carbonization temperature. With the rise of carbonization temperature, the surface carbon content will increase, but the oxygen content will decrease. After the carbon atom is replaced by the oxygen atom, tungsten oxide can stabilize the surface of tungsten carbide. The passive oxides films are formed on the surface of the pure WC, so the corrosion resistance of the WC is significantly increased [23].

RSC Advances Accepted Manuscript

3.2 Electrocatalytic activity of different catalysts

3.2.1 Polarization curves

Fig. 6 shows linear polarization curves of gas diffusion electrodes with different catalysts. The polarization curves of different electrodes are almost the same in the low potential area, indicating that the electrochemical performance of all catalysts is quite close, as seen in Fig. 6a and b. However, the electrode polarization current density of the catalyst C is higher than other electrodes in the high potential area. Thus, it can be concluded that the catalyst C has higher catalytic performance. These results indicate that the catalyst C is an active catalyst for ORR in alkaline solutions. Due to the higher specific surface area of all the samples and the presence of moderate free carbon, the catalyst C has more catalytic active center, which will facilitate the mass transportation and ensure accessibility of the reactant molecules [24]. The catalytic activity of the catalyst C is the highest in all samples. Therefore, more of amorphous carbon in WC will lower the activity of the catalysts [25], as shown in the catalyst D and catalyst E.

To further investgate the electrochemical property, activated carbon and Pt gas diffusion electrodes are used to compare its electrocatalytic activity with the prepared catalyst C. As shown in Fig. 7. Polarization measurements of all gas diffusion electrodes have no obvious distinction between -0.2 V and 0 V. In the high potential area, the polarization current density with catalyst C is higher than activated carbon and Pt gas diffusion electrodes. The current density of catalyst C gas diffusion electrode at -0.45 V is 220 $mA \cdot cm^{-2}$, which is a little higher than the Pt gas diffusion electrode with the current density of 209 $mA \cdot cm^{-2}$. Considering the high price of Pt catalyst, so it is

RSC Advances Accepted Manuscript

reasonable to believe that the WC catalyst is a good alternative to Pt catalyst.

3.2.2 Electrochemical impedance spectroscopy

Fig. 8 exhibits the EIS curves at 0.05 V (vs. SCE) with the test frequency range between 0.01 Hz and 10 kHz. The semicircle impedances show that the ORR charge transfer resistance (Rct) corresponds to the charge transfer step in neutral solution. It is clearly seen from Fig. 8a that the semicircle impedance of the catalyst C electrode is the smallest among all electrodes at the tested potential. Thus, it is reasonable to believe that the catalyst C has a better catalytic activity than other catalysts. Fig. 8b shows the corresponding Nyquist plots of the different electrodes in alkaline solution. All impedances of the electrodes present semicircles in the impedance test, which are similar to Fig. 8a. According to the size of the semicircle diameter, it can be concluded that the ORR on the catalyst C electrode is more favorable. The catalyst C shows better catalytic activity resulted from the enhanced reaction kinetics [26]. The results of the electrochemical impedance test show that the amorphous carbon content has an important effect on the catalytic activity of WC, which is consistent with the experimental polarization curves.

4. Conclusions

In summary, this work successfully parpared mesoporous WC with a high catalytic activity and specific surface area by the low temperature combustion synthesis method. With the rise of carbonization temperature, the amorphous carbon content of the prepared WC will increase. The presence of a moderate amount of oxygen is beneficial to improve the stability of the tungsten carbide. The as-prepared mesoporous

RSC Advances Accepted Manuscript

WC nanoparticles exhibit excellent performance for ORR, mainly due to the free carbon content and morphological characteristics of the mesoporous materials. This study clearly indicates that the amorphous carbon has an important effect on the catalytic activity of WC catalysts.

Acknowledgments

Ping Li and Fuqiang Zhai thanks China Scholarship Council (CSC) for providing the scholarship.

References

[1] H. Meng and P. K. Shen. Electrochem. commun, 2006, 8, 588-594.

[2] H. Meng and P. K. Shen. Chem. Commun, 2005, 1, 4408-4410.

[3] M. Nie, H. L. Tang, Z. D. Wei, S. P. Jiang and P. K. Shen. Electrochem. Commun, 2007, 9, 2375-2379.

[4] G. J. K. Acres, J. C. Frost, G. A. Hards, R. J. Poter, T. R. Ralph, D. Thompsett, G. T. Burstein and G. J. Hutchings. Catal. Today, 1997, 38, 393-400.

[5] R.B. Levy and M. Boudart. Science, 1973, 181, 547-549.

[6] Z. J. Mellinger, T. G. Kelly and J. G. Chen. ACS. Catal, 2012, 2, 751-758.

[7] M. B. Zellner, J. G. Chen. J. Catal, 2005, 235, 393-402.

[8] H. Chhina, S. Campbell and O. Kesler. J. Power Sources, 2007, 164, 431-440.

[9] E. C. Weigert, A. L. Stottlemyer, M. B. Zellner and G. C. Jingguang. J. Phys. Chem. C, 2007, 111, 14617-14620.

[10] Z. Zhao, X. Fang, Y. Li, Y. Wang, P. K. Shen, F. Xie and X. Zhang. Electrochem. Commun, 2009, 11, 290-293.

RSC Advances Accepted Manuscript

[11] J. Lemaitre, B. Vidick and B. Delmon. J. Catal, 1986, 99, 415-427.

[12] B. Vidick, J. Lemaitre and B. Delmon. J. Catal, 1986, 99, 428-438.

[13] G. Leclercq, M. Kamal, J. F. Lamonier, L. Feigenbaum, P. Malfoy and L. Leclercq. Appl. Catal. A, 1995, 121, 169-190.

[14] G. Leclercq, M. Kamal, J. M. Giraudon, P. Devassine, L. Feigenbaum, L. Leclercq, A. Frennetb, J. M. Bastinb, A. Löfbergb, S. Deckerb and M. Dufourb. J. Catal, 1996, 158, 142-169.

[15] Y. Hara, N. Minami and H. Itagaki. Appl. Catal. A, 2007, 323, 86-93.

[16] J. P. Bosco, K. Sasaki, M. Sadakane, W. Ueda and J. G. Chen. Chem. Mat, 2010, 22, 966-973.

[17] D. J. Ham, R. Ganesan and J. S. Lee. Int. J. Hydrogen. Energy, 2008, 33, 6865-6872.

[18] Z. Fu, Q. M. Huang, X. D. Xiang, Y. L. Lin, W. Wu, S. J. Hu and W. S. Li. Int. J. Hydrogen. Energy, 2012, 37, 4704-4709.

[19] P. Li, Z. W. Liu, L. Q. Cui, F. Q. Zhai, Q. Wan, Z. L. Li, Z. Z. Fang, A. A. Volinsky and X. H. Qu. T. Int. J. Hydrogen. Energy, 2014, 39, 10911-10920.

[20] J. F. Drillet, H. Bueb, U. Dettlaff-Weglikowska, R. Dittmeyer and S. Roth. J. Power Sources, 2010, 195, 8084-8088.

[21] C. Tran, X.Q. Yang and D. Qu. J. Power Sources, 2010, 195, 2057-2063.

[22] C.A. Ma, W. M. Zhang, G. H. Li, Y. F. Zheng, B. X. Zhou and D. H. Cheng. Acta Chim. Sinica, 2005, 63, 1151-1154.

[23] K. C. Lee, A. Ishihara, S. Mitsushima, N Kamiyaa and K. Ota. Electrochim. Acta,

RSC Advances Accepted Manuscript

2004, 49, 3479-3485.

[24] H. Zheng, Z. Chen and Y. Li. Electrochim. Acta, 2013, 108, 486-490.

[25] X. Yang, Y. C. Kimmel, J. Fu, B. E. Koel and J. G. Chen. ACS. Catal, 2012, 2, 765-769.

[26] E. H. Yu, K. Scott and R. W. Reeve. J. Electroanal. Chem, 2003, 547, 17-24.

RSC Advances Accepted Manuscript

Figure captions

Fig. 1. X-ray diffraction patterns of the tungsten carbide synthesized at different carbonization temperatures.

Fig. 2. FESEM micrographs of the products of WC: (a) catalyst A; (b) catalyst B; (c) catalyst C; (d) catalyst D and (e) catalyst E.

Fig. 3. N_2 adsorption-desorption isotherms of the catalyst C sample (inset: BJH pore size distribution).

Fig. 4. DG-DTA curves of the catalyst C.

Fig. 5. XPS spectra of the catalyst A: (a) C 1s peak and (b) W4f peak.

Fig. 6. Linear polarization curves of gas diffusion electrodes with different catalysts (A, B, C, D, E): (a) neutral solution and (b) alkaline solution.

Fig. 7. Linear polarization curves of gas diffusion electrodes with catalyt C, Pt and activated carbon in the neutral solution.

Fig. 8. Impedance spectra of gas diffusion electrodes with different catalysts (A, B, C, D, E); (a) neutral solution and (b) alkaline solution.

Table captions

Table 1. The BET and carbon content of the products.

Table 2. The surface elements content of different products.

RSC Advances Accepted Manuscript

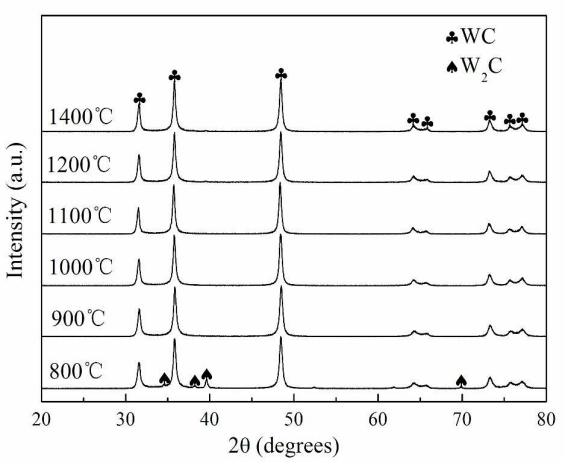

Fig. 1

RSC Advances Accepted Manuscript

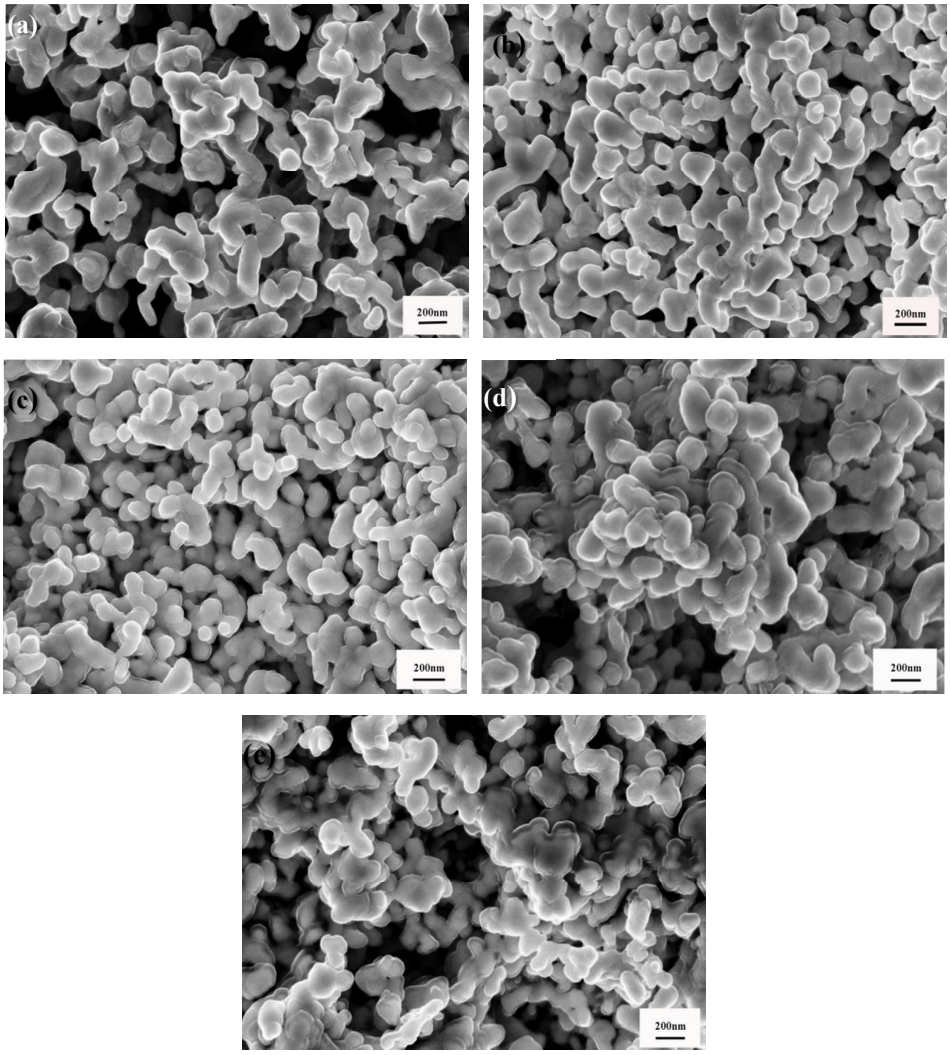

Fig. 2

RSC Advances Accepted Manuscript

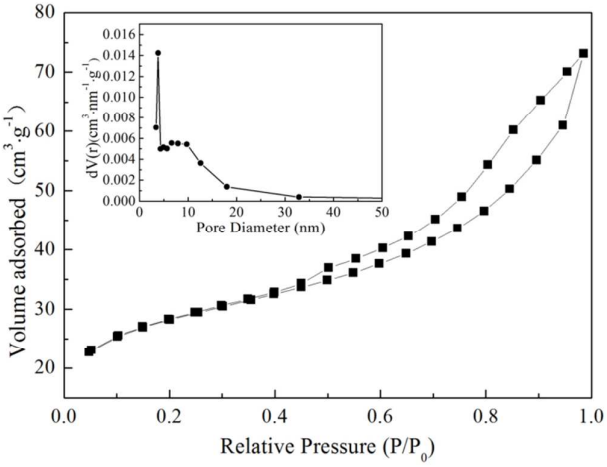

Fig. 3

RSC Advances Accepted Manuscript

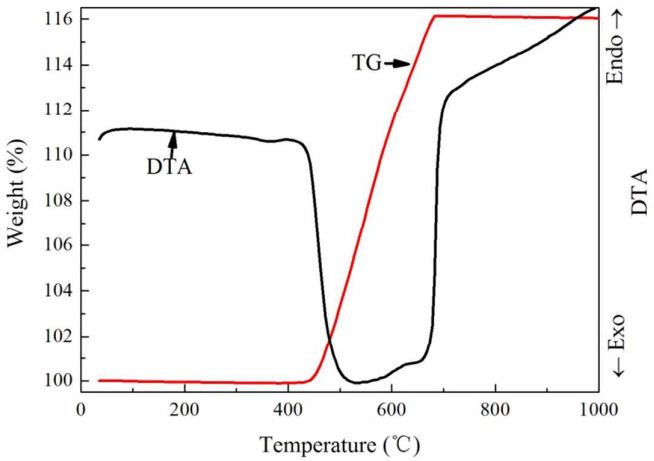

Fig. 4

RSC Advances Accepted Manuscript

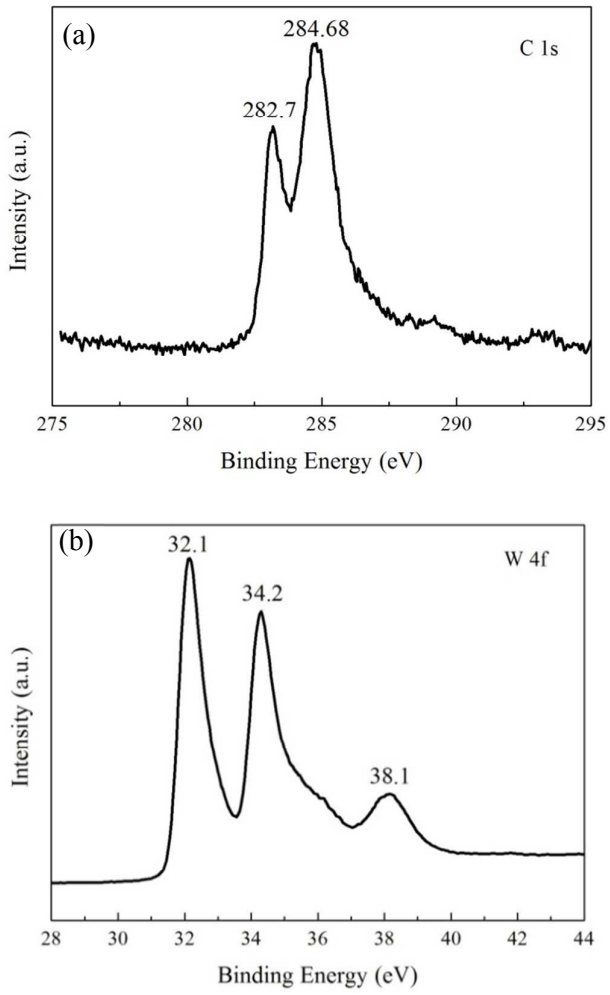

Fig. 5

RSC Advances Accepted Manuscript

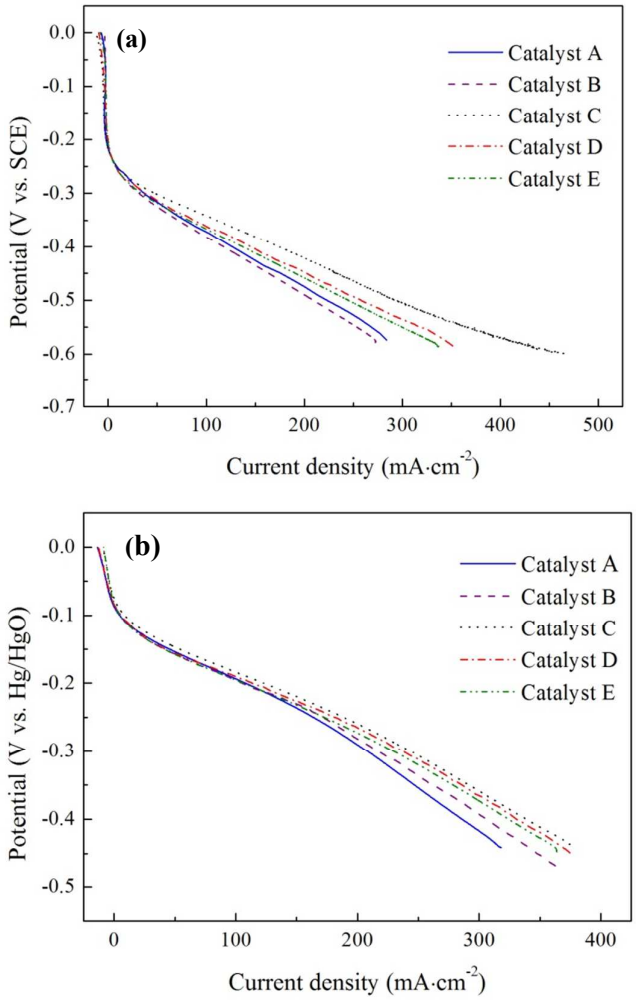

Fig. 6

RSC Advances Accepted Manuscript

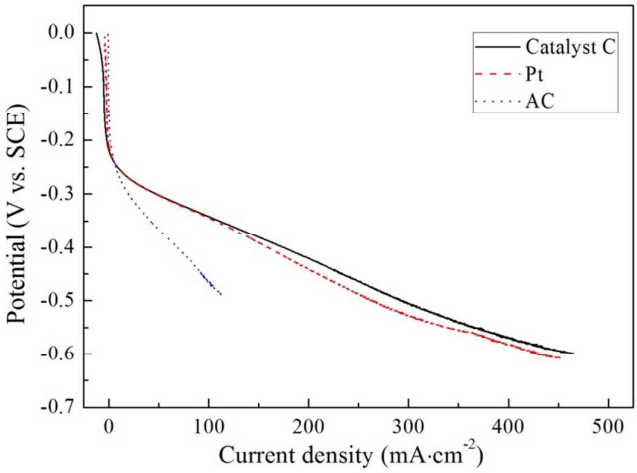

Fig. 7

RSC Advances Accepted Manuscript

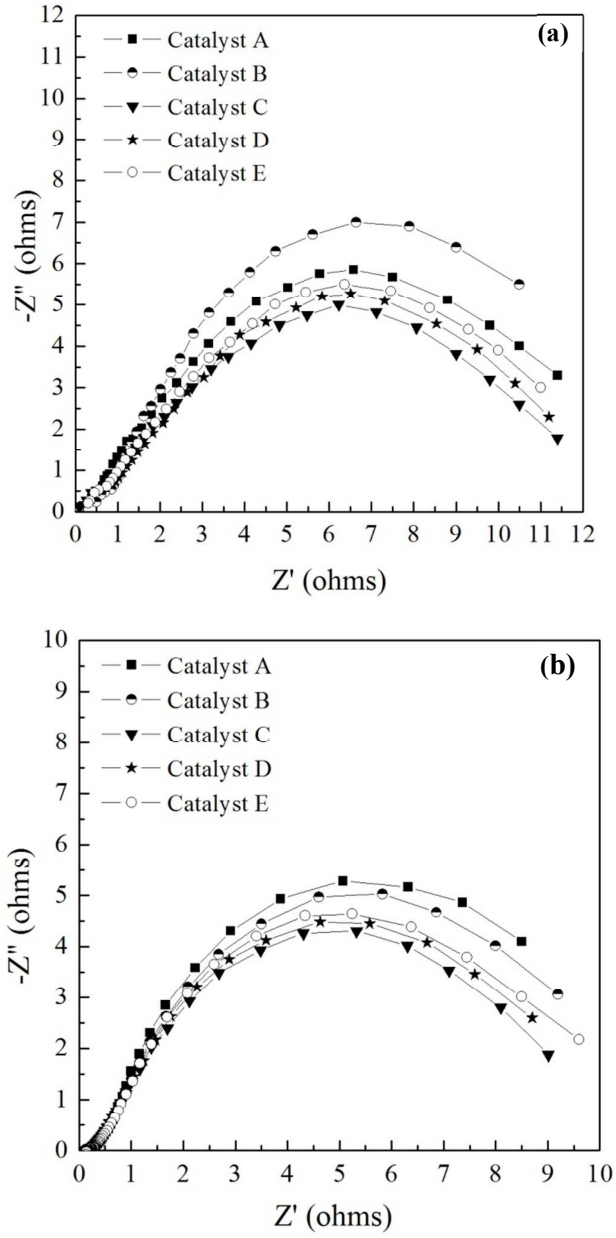

Fig. 8

RSC Advances Accepted Manuscript

Table 1. The BET and carbon content of the products.

The products	C wt.% in the product	Free carbon wt.% in the product	BET ($m^2 \cdot g^{-1}$)
Catalyst A	6.66	0.54	19.754
Catalyst B	6.70	0.58	24.342
Catalyst C	7.10	0.98	41.297
Catalyst D	8.62	2.50	36.612
Catalyst E	8.66	2.54	31.295

RSC Advances Accepted Manuscript

Table 2. The surface elements content of different products.

The products	Atomic content (mole percentage, %)		
	C	W	O
Catalyst A	38	34	28
Catalyst B	40	34	26
Catalyst C	48	35	17
Catalyst D	53	35	12
Catalyst E	55	35	10

RSC Advances Accepted Manuscript

Nanostructured tungsten carbide is used as the catalyst for the gas diffusion electrode. The presence of the 0.98 wt % amorphous carbon is beneficial for improving the conductivity and dispersibility of tungsten carbide catalyst.

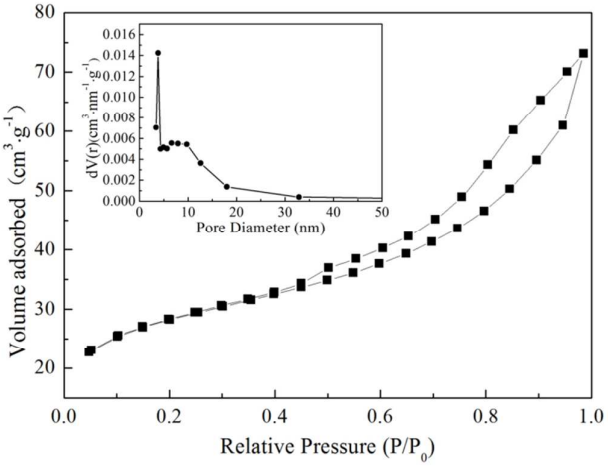

RSC Advances Accepted Manuscript